Imaging of Single Molecules at the European XFEL

“Start-to-End” Simulations

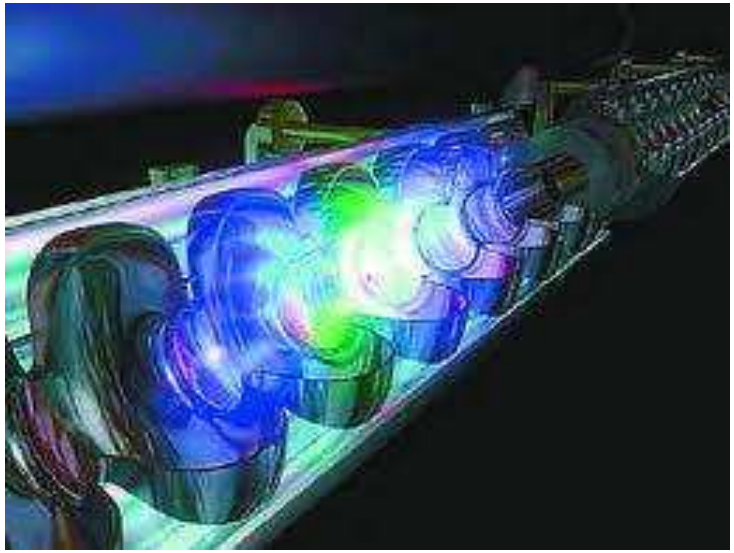

Igor Zagorodnov

S2E Meeting

DESY
10. February 2014

HELMHOLTZ GEMEINSCHAFT

DESY

S2E Simulations of Bioimaging

Perspectives of Imaging of Single Protein Molecules with the Present Design of the European XFEL

Svitozar Serkez , [a,1] Vitali Kocharyan, [a] Evgeni Saldin, [a]
Igor Zagorodnov, [a] Gianluca Geloni, [b]
and Oleksandr Yefanov [c]

Start to end simulations from the electron injector at the beginning of the accelerator complex to the biomolecule electron-density reconstruction indicate that one can achieve diffraction without destruction at near-atomic resolution with 10^{13} photons in a 4 fs pulse at 4 keV photon energy and in a 100 nm focus, corresponding to a fluence of 10^{23}ph/cm^2. This result is exemplified using the RNA Pol II molecule as a case study.

S2E Simulations of Bioimaging

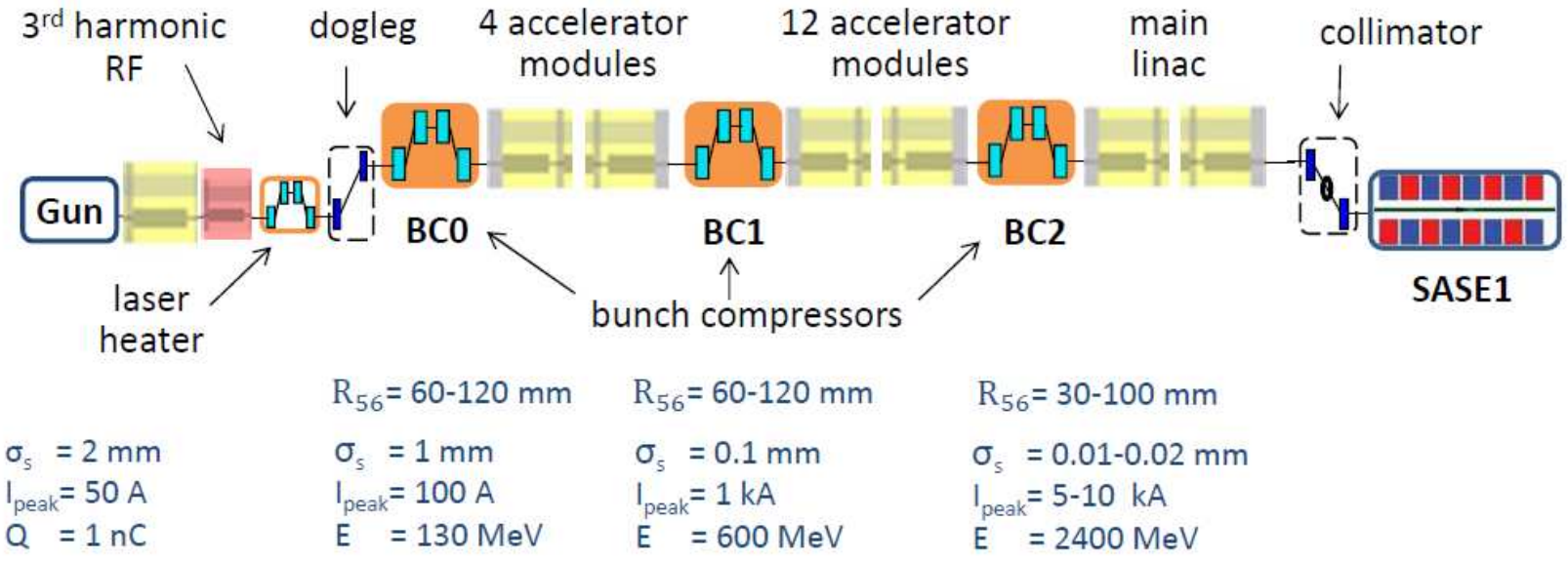

Fig. 1. Sketch of the European XFEL bunch compression system.

S2E Simulations of Bioimaging

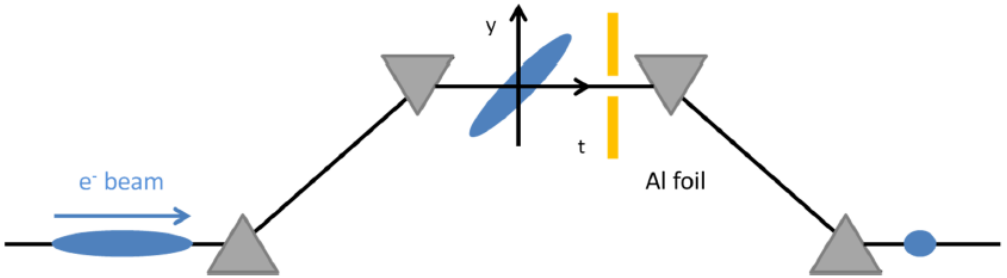

Fig. 2. Sketch of an electron bunch at the center of the BC2 magnetic bunch compressor chicane.

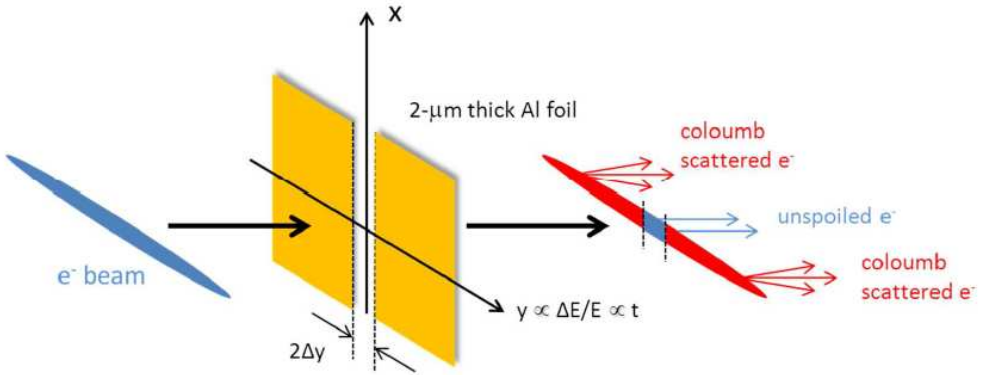

Fig. 3. The slotted foil at chicane center generates a narrow, unspoiled beam center

S2E Simulations of Bioimaging

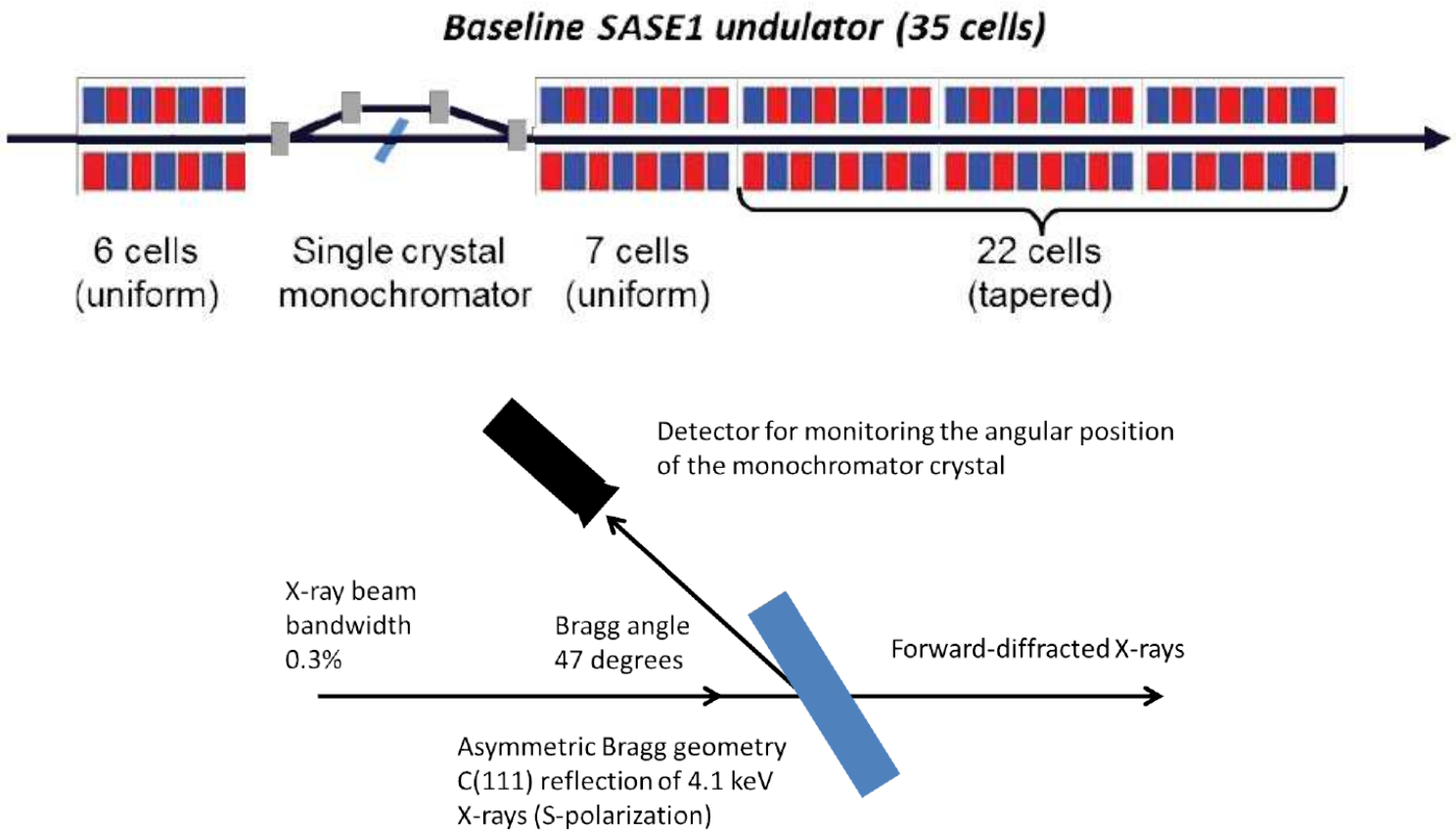

Fig. 5. Schematic of the single crystal monochromator for operation in the photon energy range around 4 keV.

S2E Simulations of Bioimaging

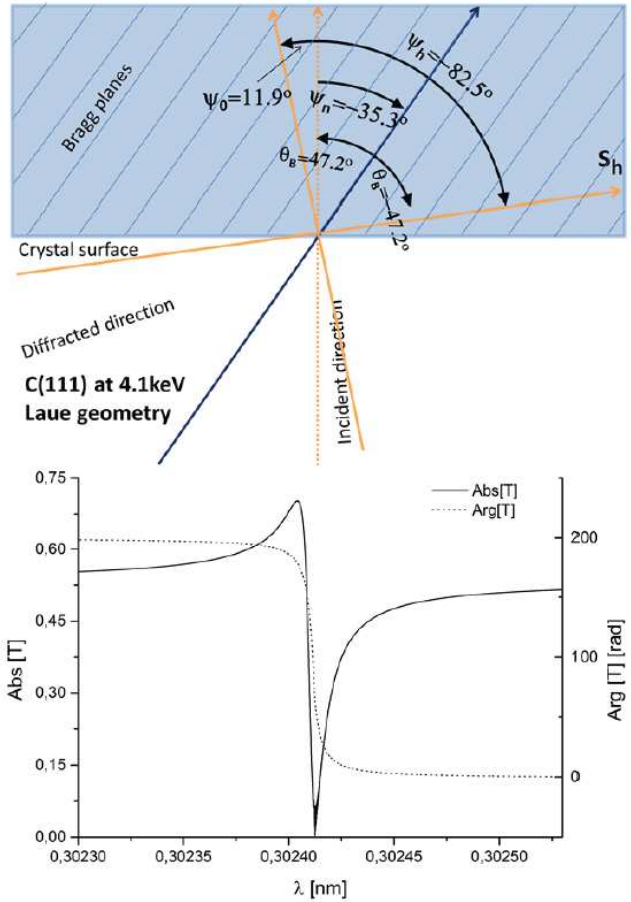

Fig. 7. Upper plot: scattering geometry (we are following the notation in [59]). Lower plot: modulus and phase of the transmittance for the C(111) asymmetric Laue reflection from the diamond crystal in Fig. 6 at 4.1 keV.

S2E Simulations of Bioimaging

Fig. 8. Layout of the optical components for the SPB beamline.

The Single Particles, Clusters and Biomolecules (SPB) instrument at the European XFEL is located behind the SASE1 undulator, and aims to support imaging and structure determination of biological specimen between about 0.1μm and 1μm size.

S2E Simulations of Bioimaging

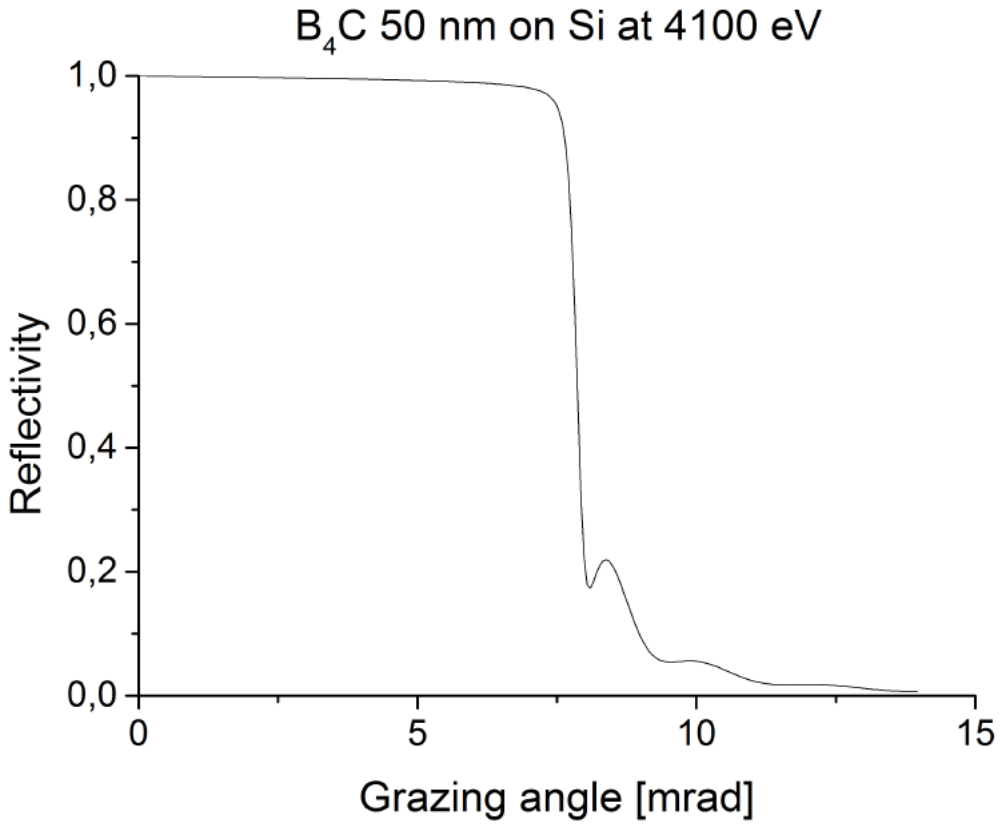

Fig. 9. reflectivity of a 50 nm perfect B_4C substrate on *Si* substrate at 4.1 keV as a function of the grazing angle. Calculation are done via the web interface [61].

S2E Simulations of Bioimaging

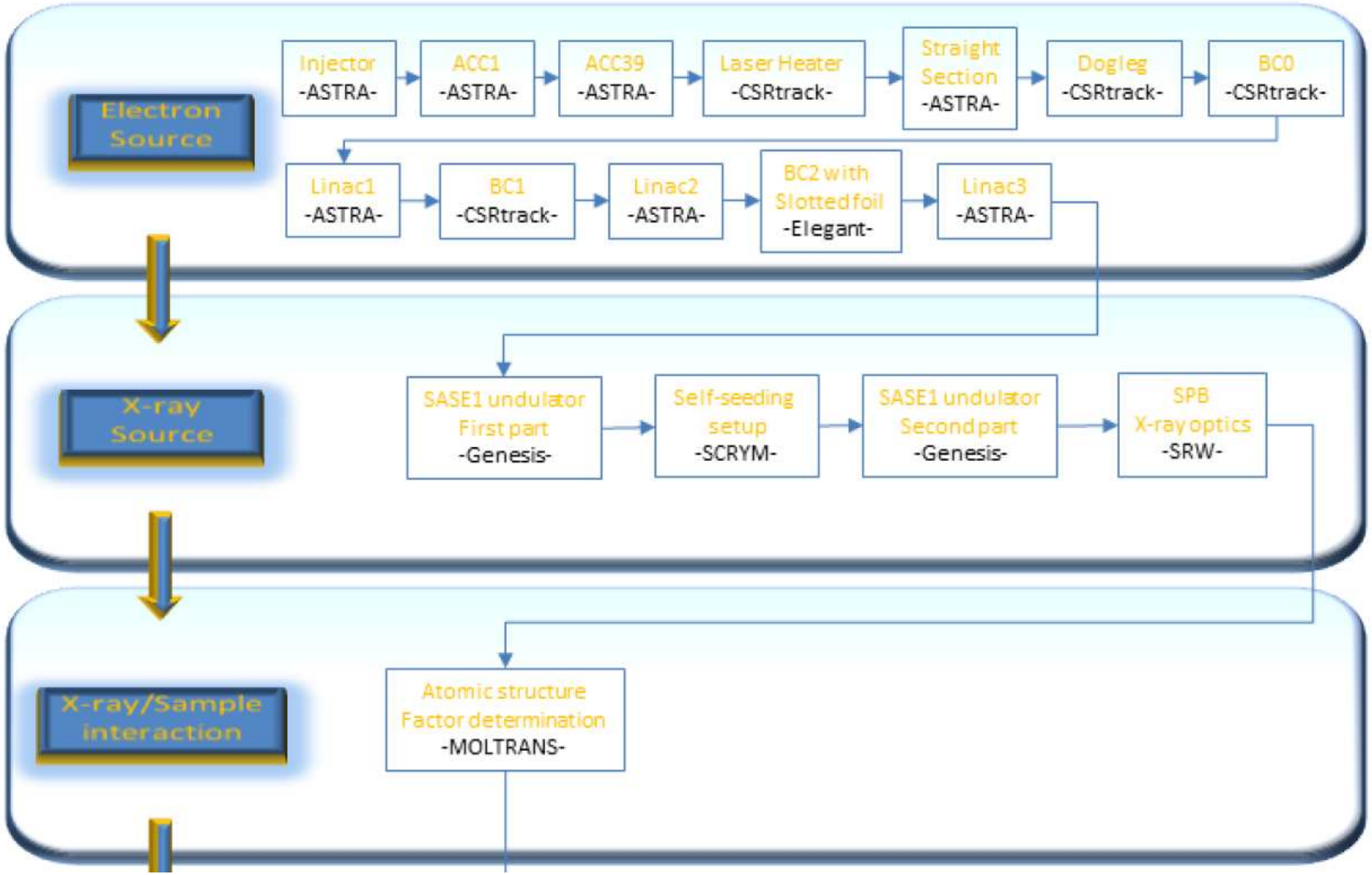

S2E Simulations of Bioimaging

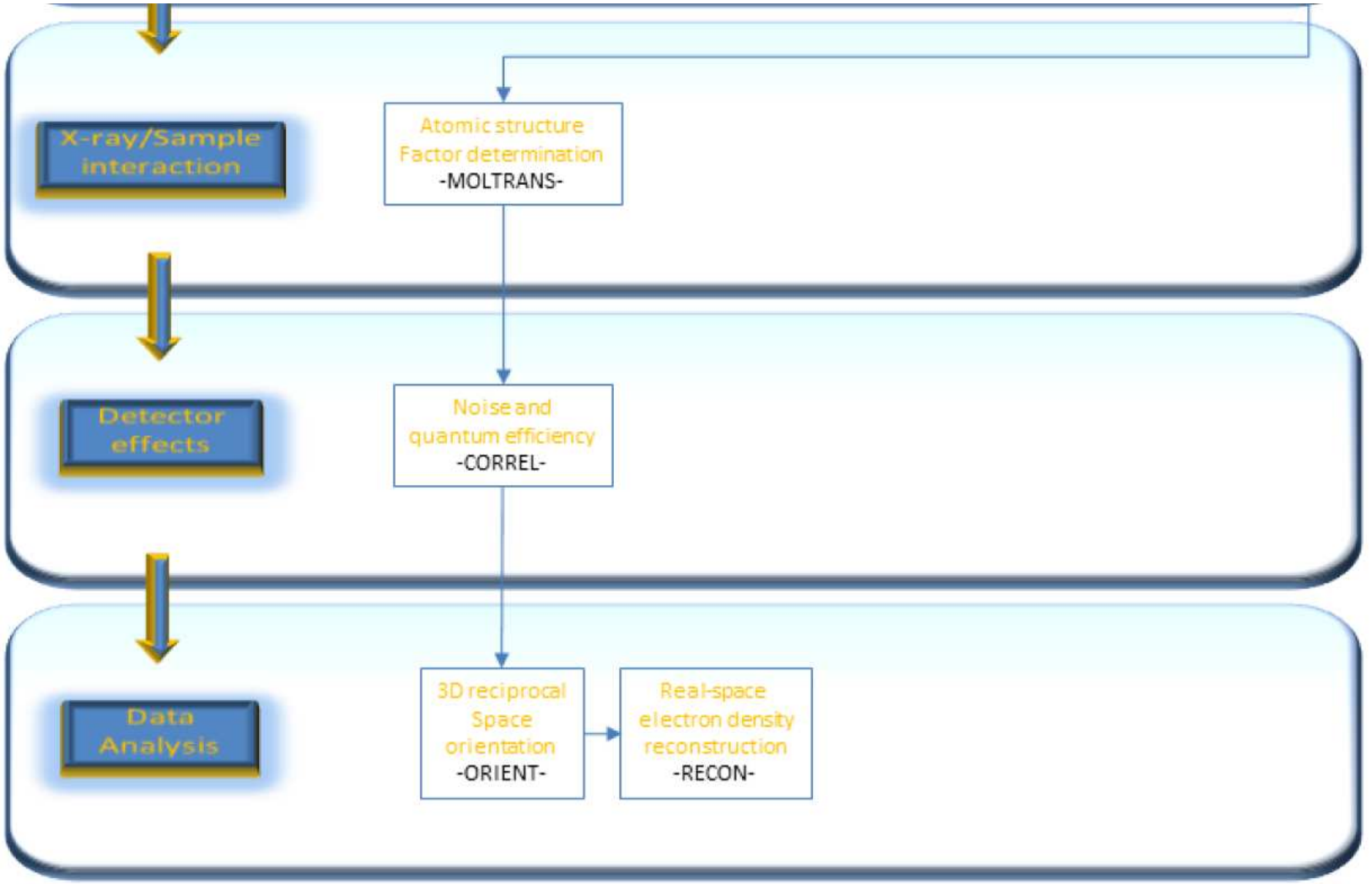

S2E Simulations of Bioimaging

Comparison CSRtrack vs Elegant

(we are going to simulate the foil effect in Elegant)

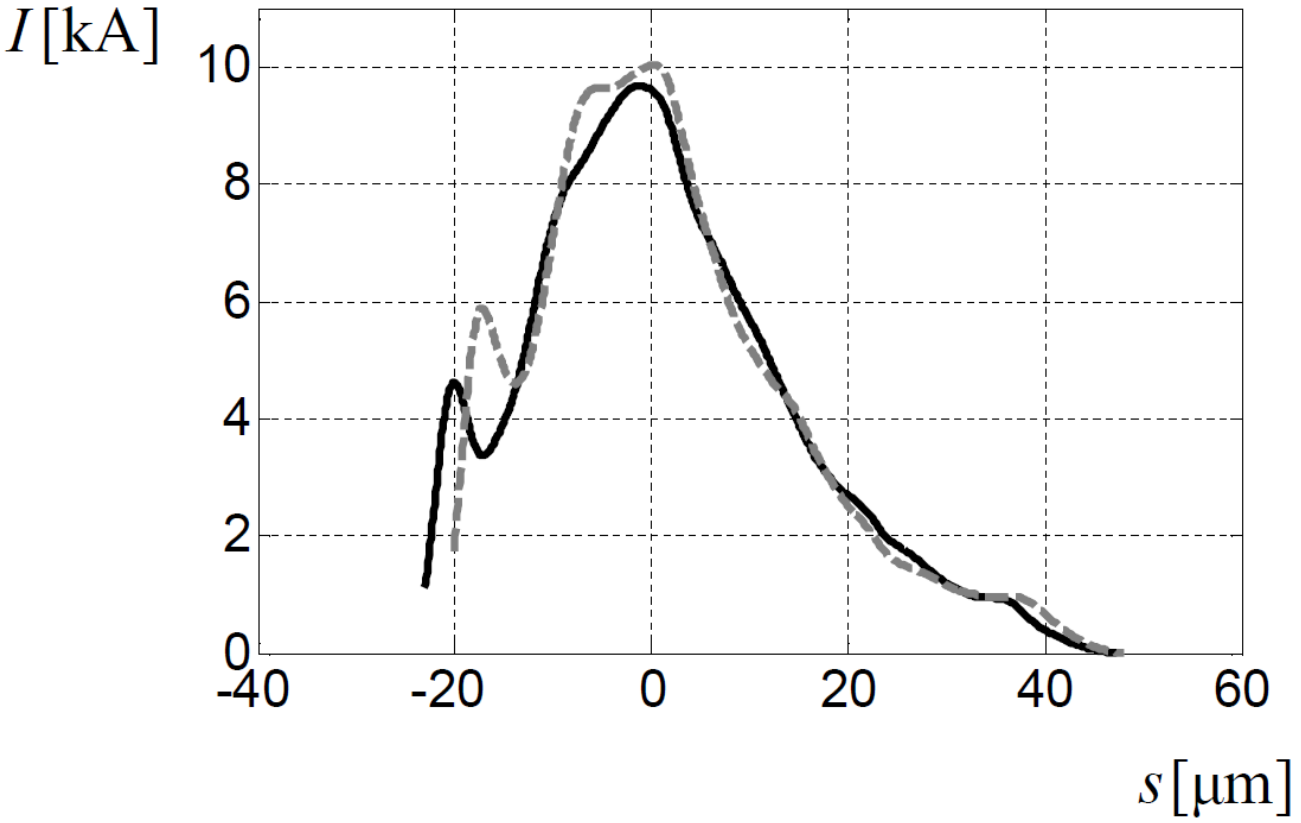

S2E Simulations of Bioimaging

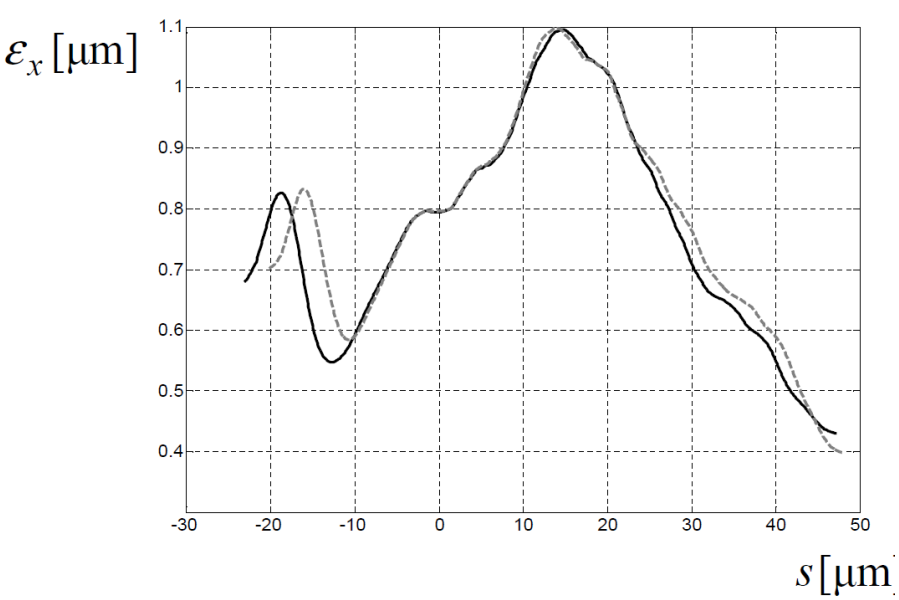

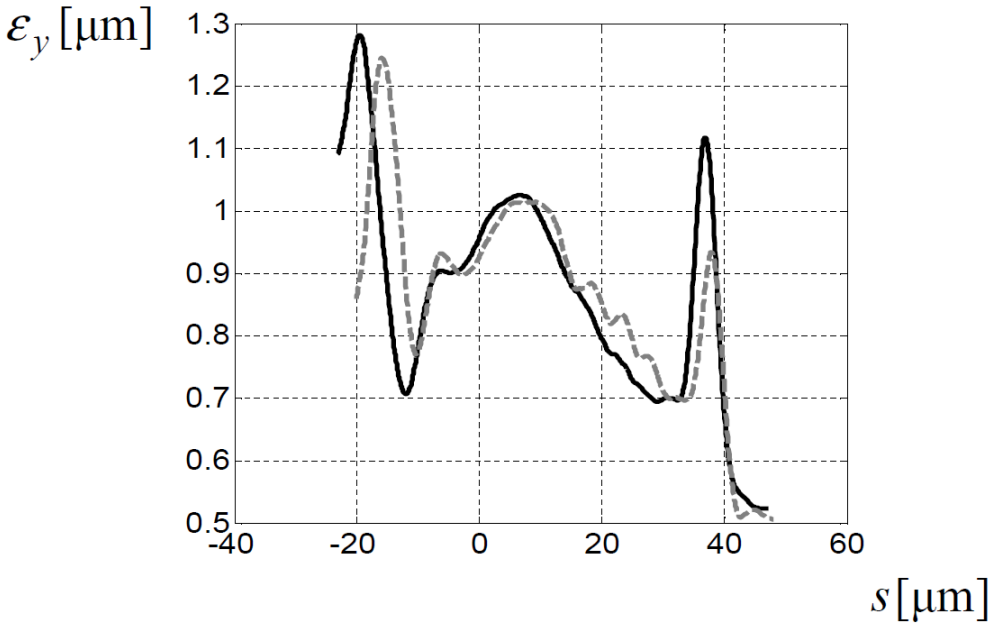

S2E Simulations of Bioimaging

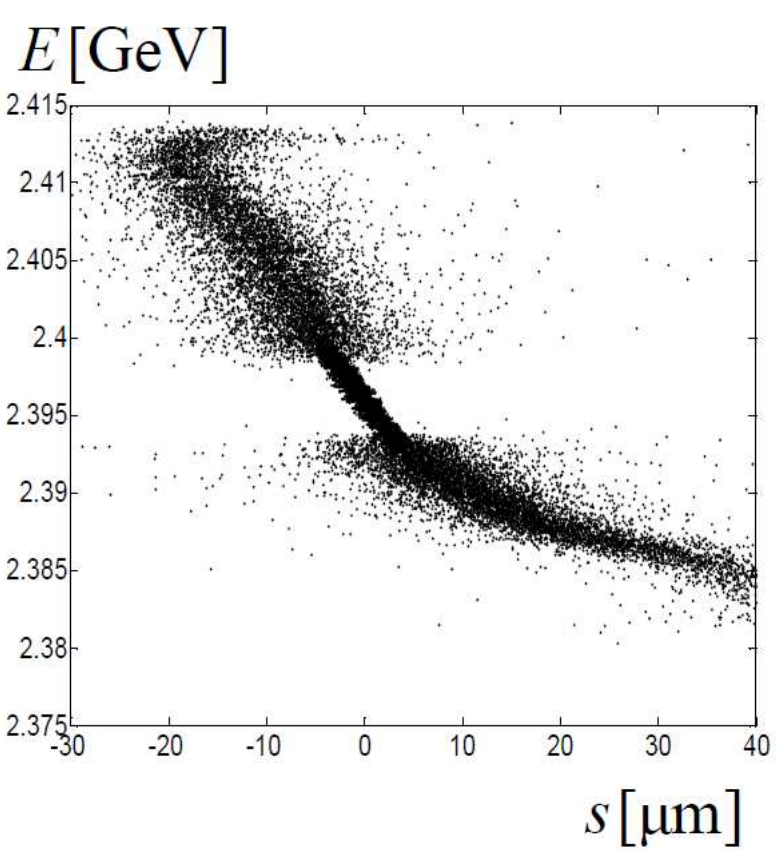

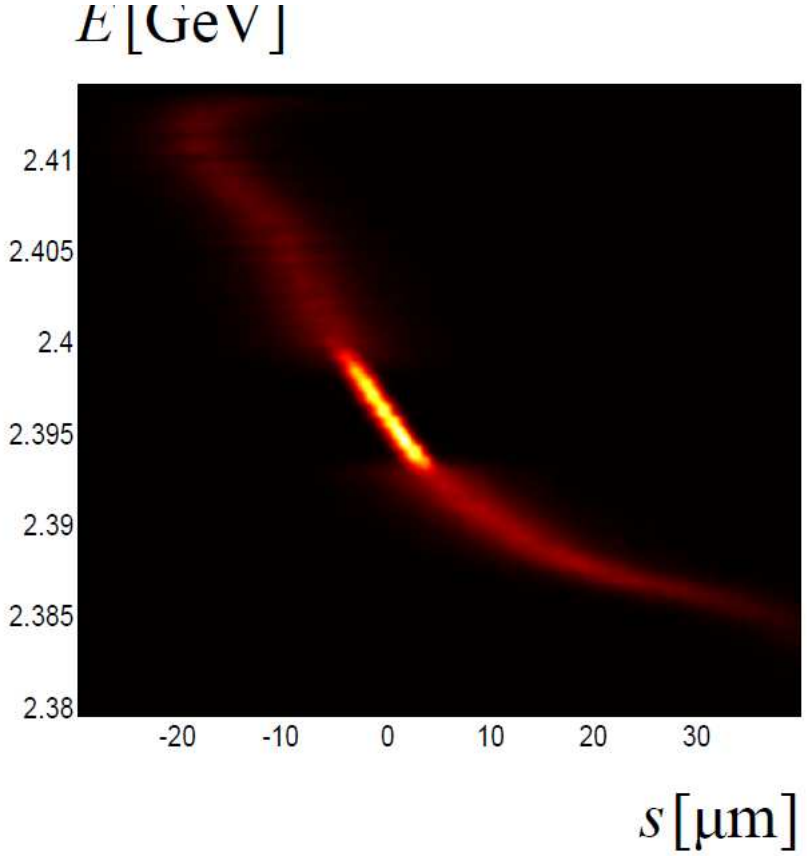

S2E Simulations of Bioimaging

Let us consider the slice properties as well

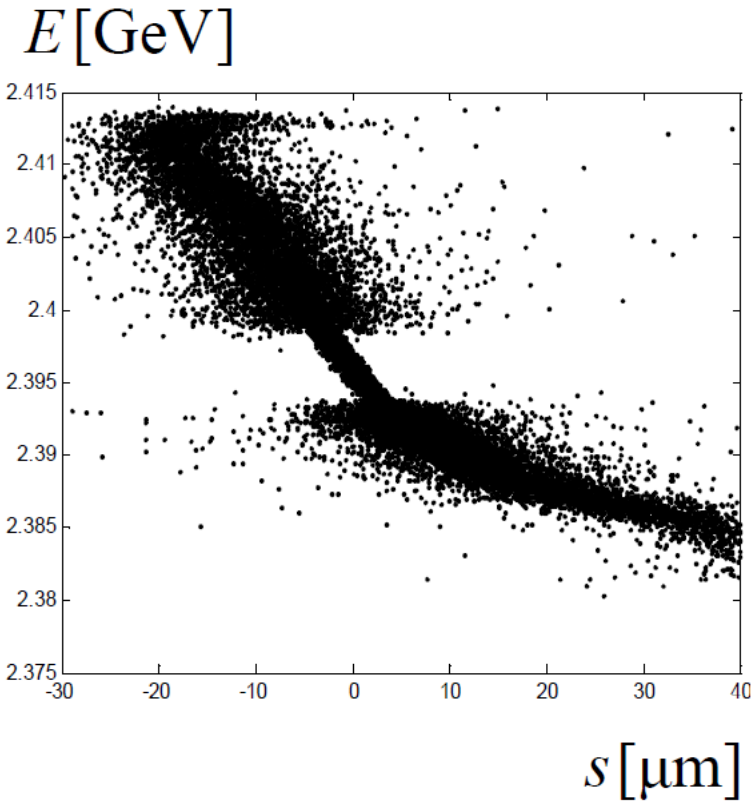

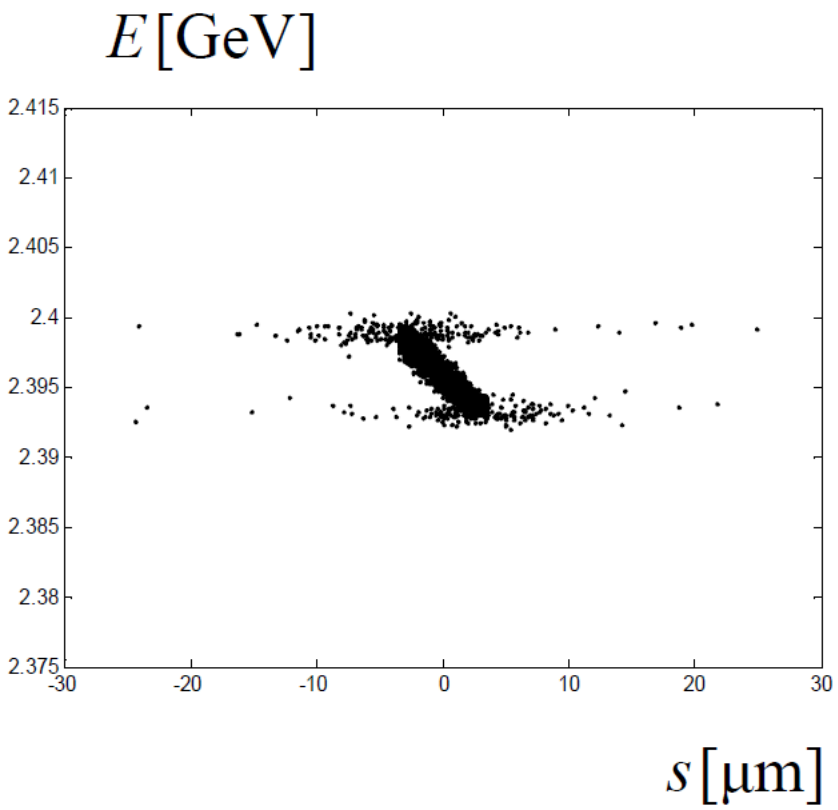

S2E Simulations of Bioimaging

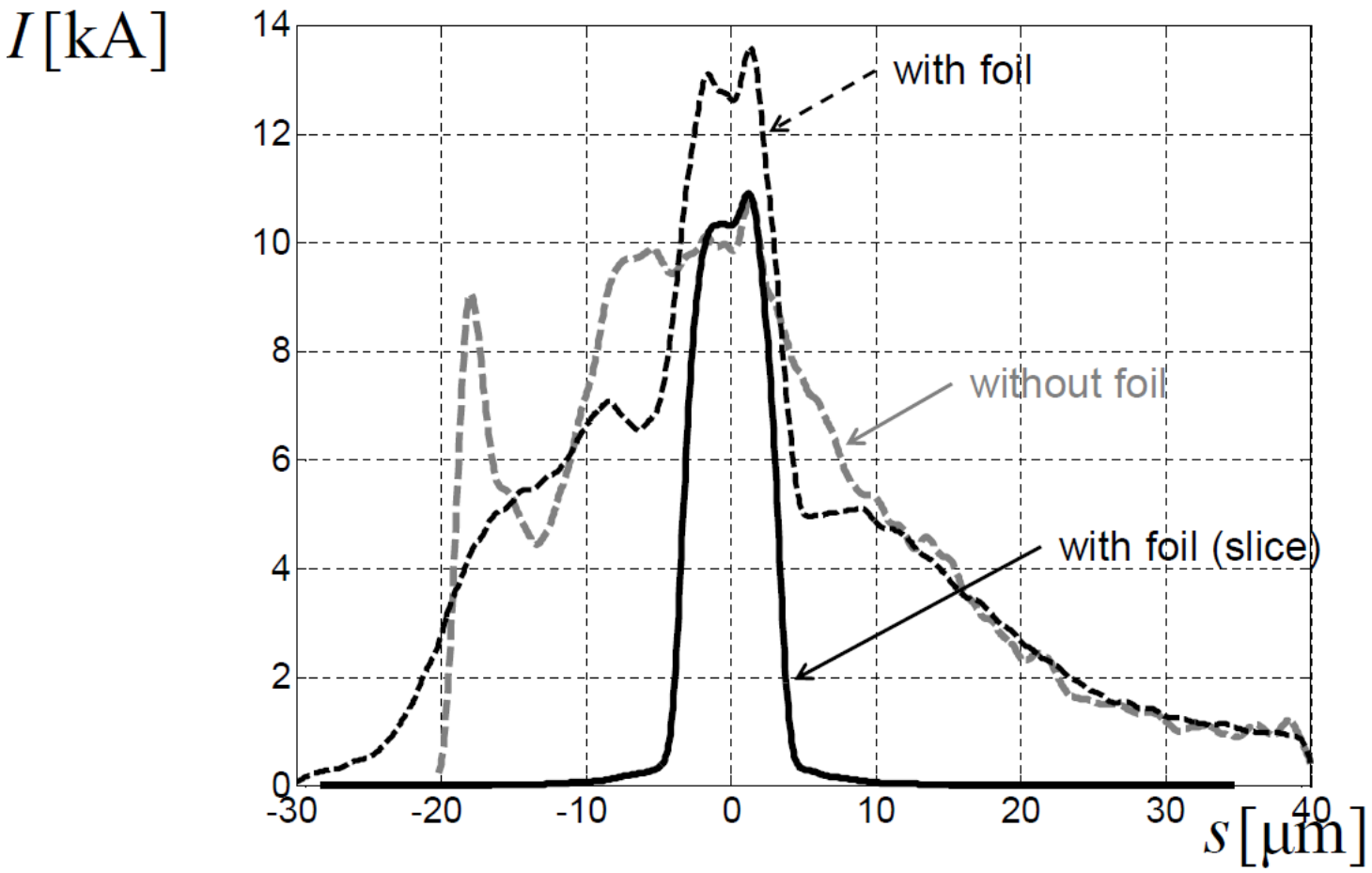

S2E Simulations of Bioimaging

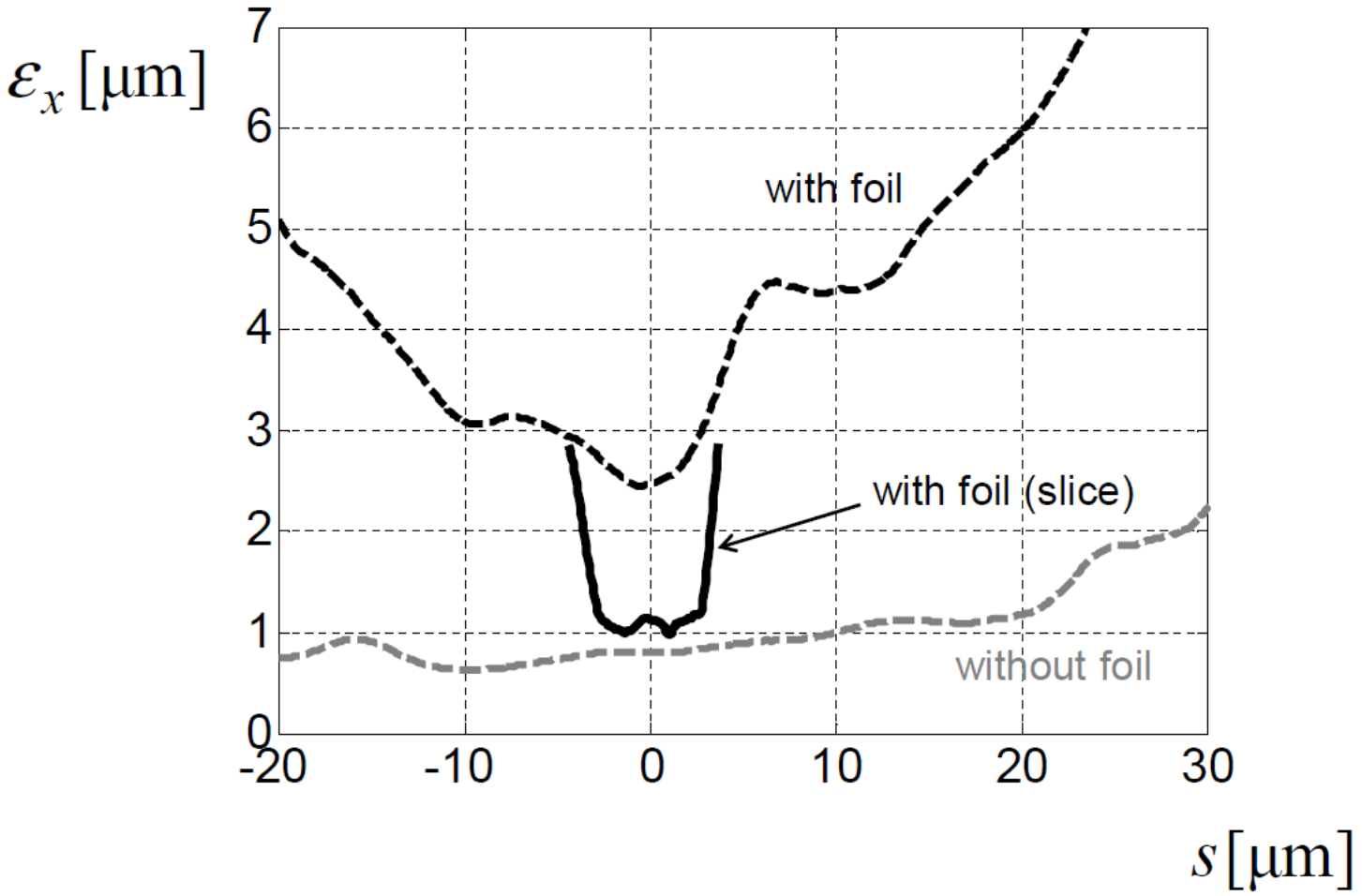

S2E Simulations of Bioimaging

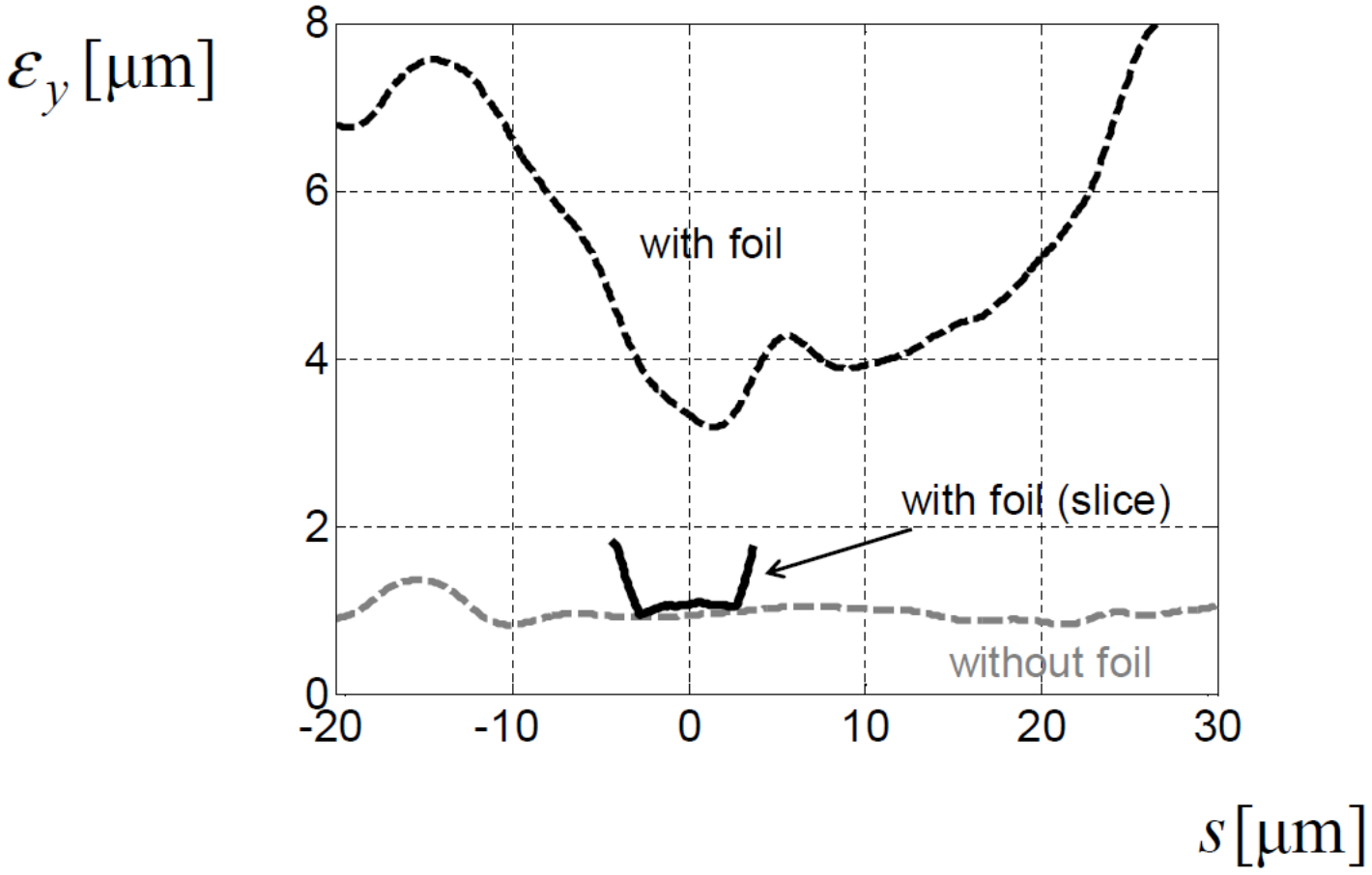

S2E Simulations of Bioimaging

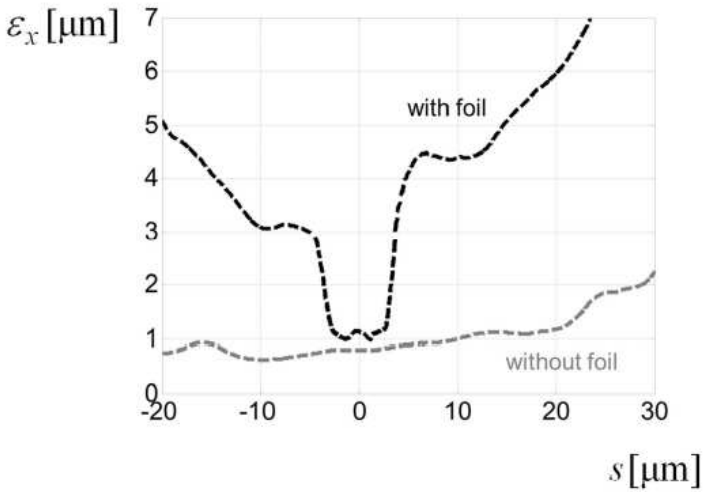

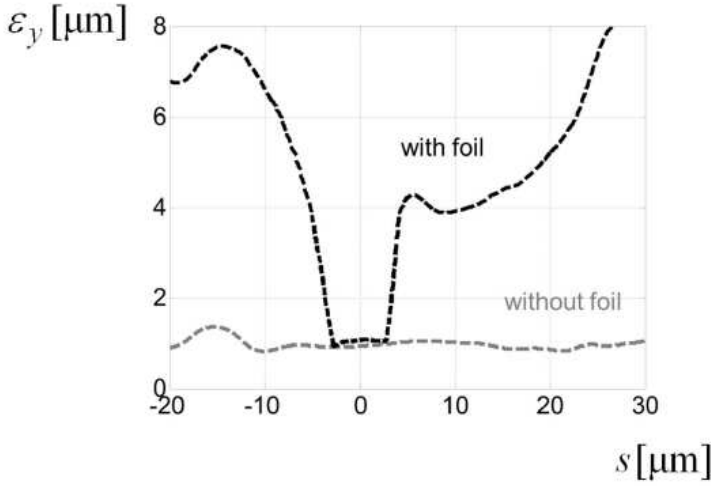

Fig. 13. Left plot: Vertical normalized emittance as a function of the position inside the electron bunch after BC2. The grey dashed curve is from particle tracking without foil. The black dashed curve is from particle tracking with foil. Right plot: Horizontal emittance as a function of the position inside the electron bunch after BC2. The grey dashed curve is from particle tracking without foil. The black dashed curve is from particle tracking with foil. (In both plots we removed 6 % of strongly scattered particles from the analysis.)

S2E Simulations of Bioimaging

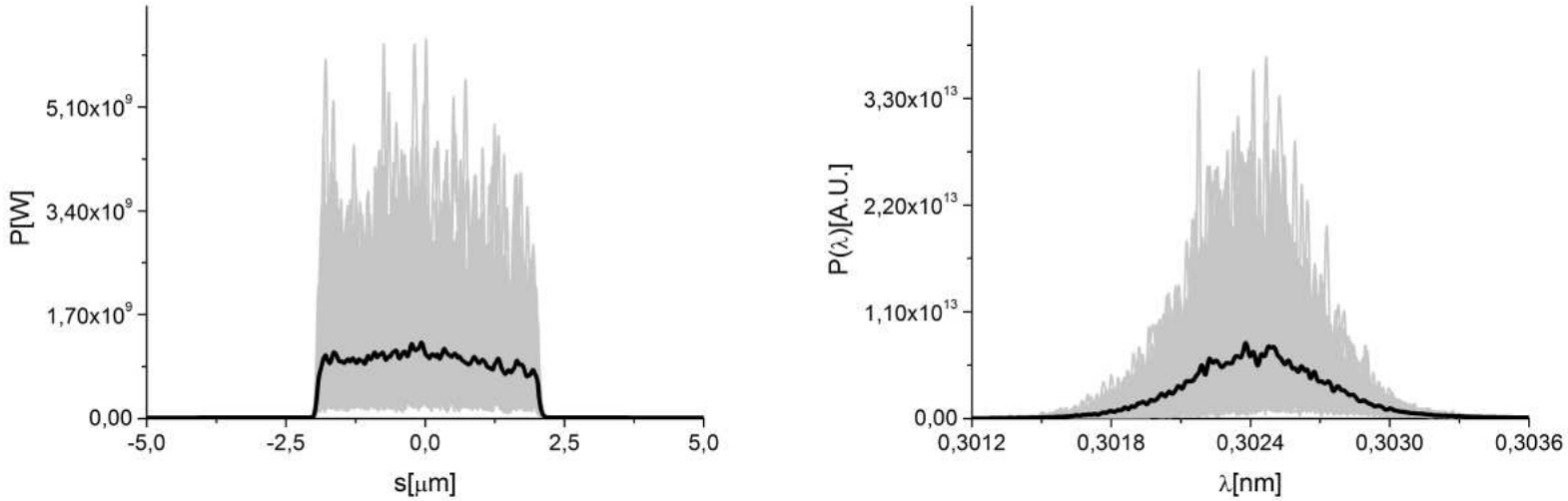

Fig. 15. Power distribution and spectrum of the SASE x-ray pulse at the exit of the first undulator for the case of long (12 fs) pulse mode of operation.

S2E Simulations of Bioimaging

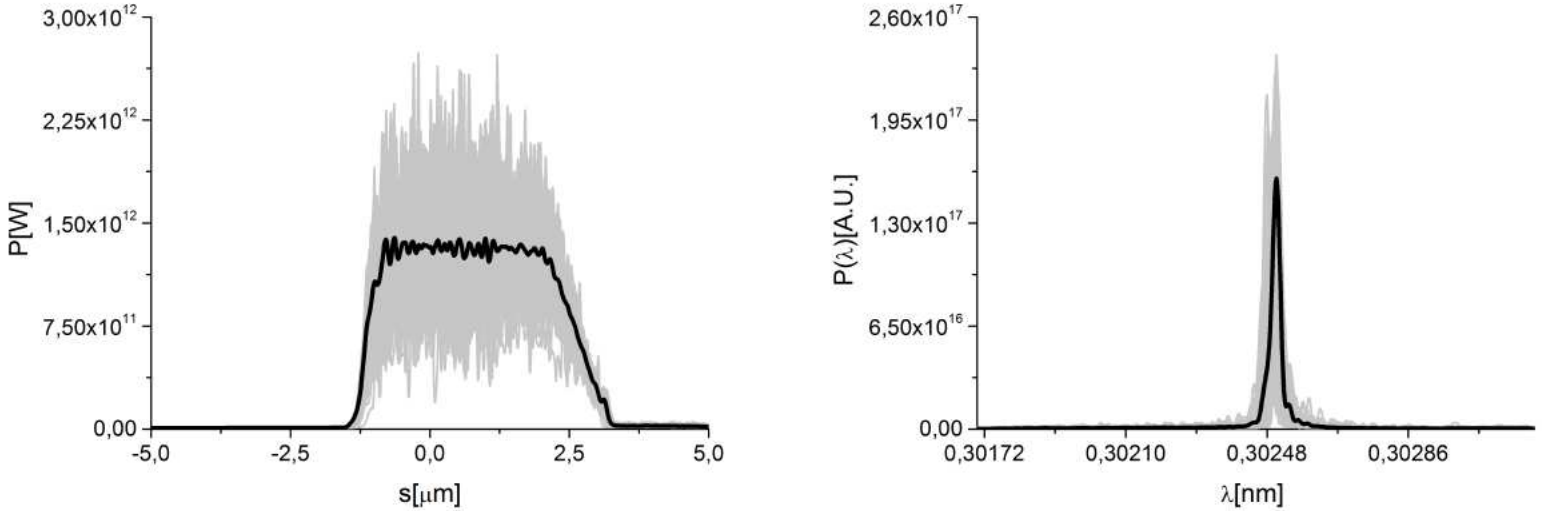

Fig. 17. Power distribution and spectrum of the output radiation pulse for the case of long (12 fs) pulse mode of operation.

S2E Simulations of Bioimaging

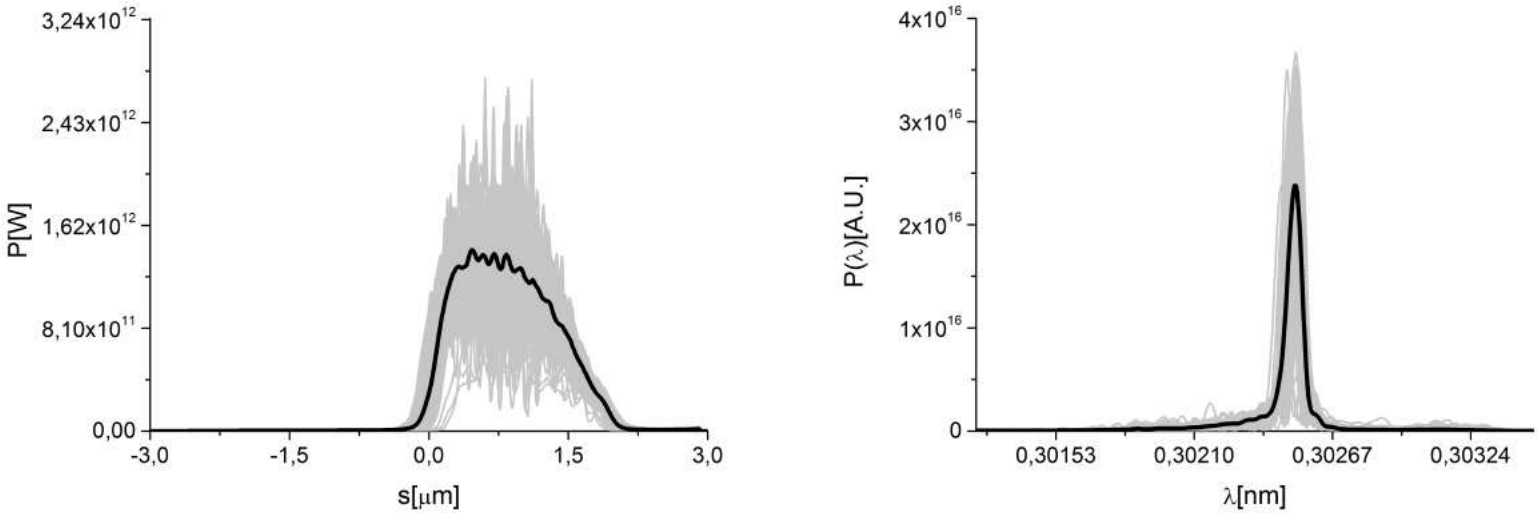

Fig. 21. Power distribution and spectrum of the output radiation pulse for the case of short (4 fs) pulse mode of operation.

S2E Simulations of Bioimaging

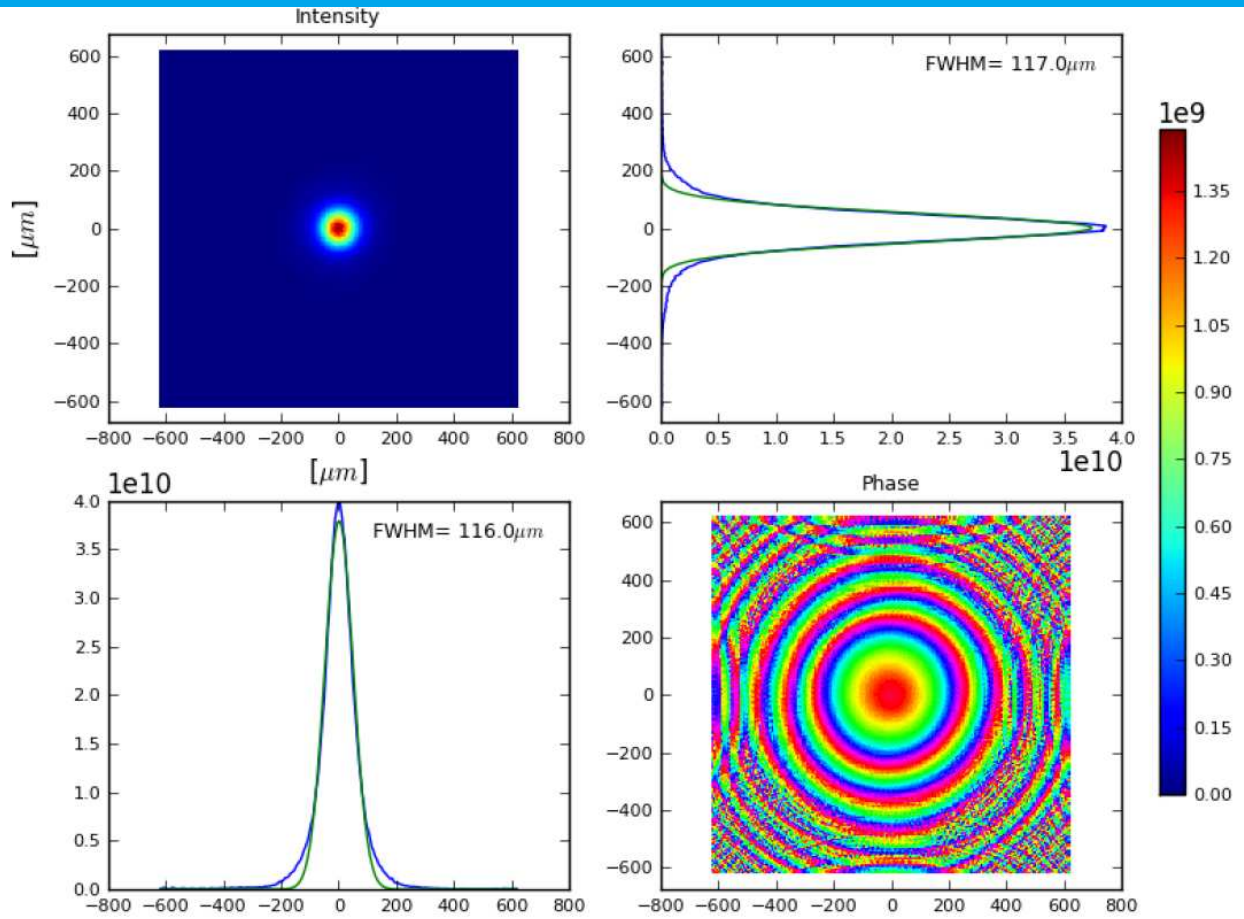

Fig. 25. Upper plot. Calculated intensity and phase distribution of the FEL beam at the exit of SASE 1 undulator. Results refer a longitudinal position inside the radiation pulse roughly corresponding to the maximum power value. Lower plot.

S2E Simulations of Bioimaging

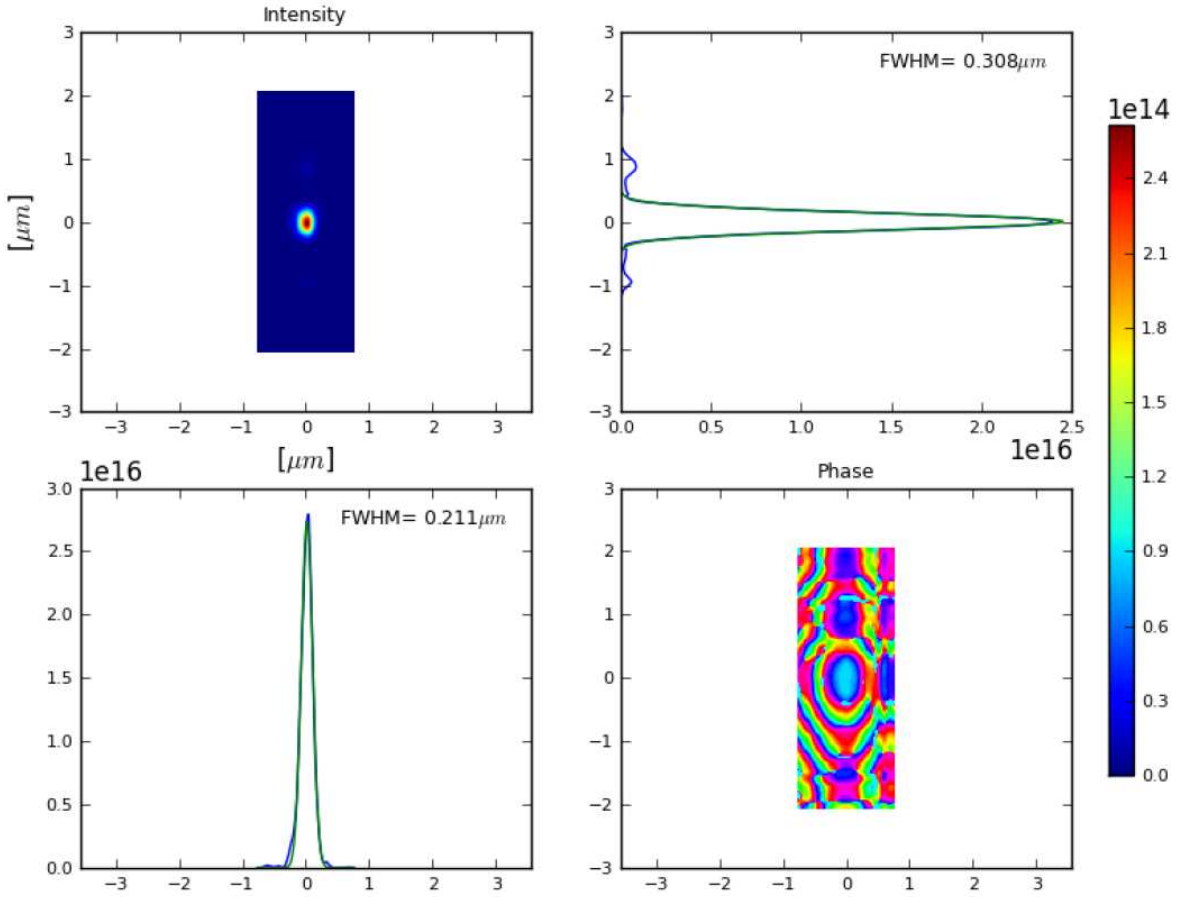

Fig. 29. Upper plot. Calculated intensity and phase distribution of the FEL beam in the focus. Results refer a longitudinal position inside the radiation pulse roughly corresponding to the maximum power value. Lower plot. Distribution of the radi-

S2E Simulations of Bioimaging

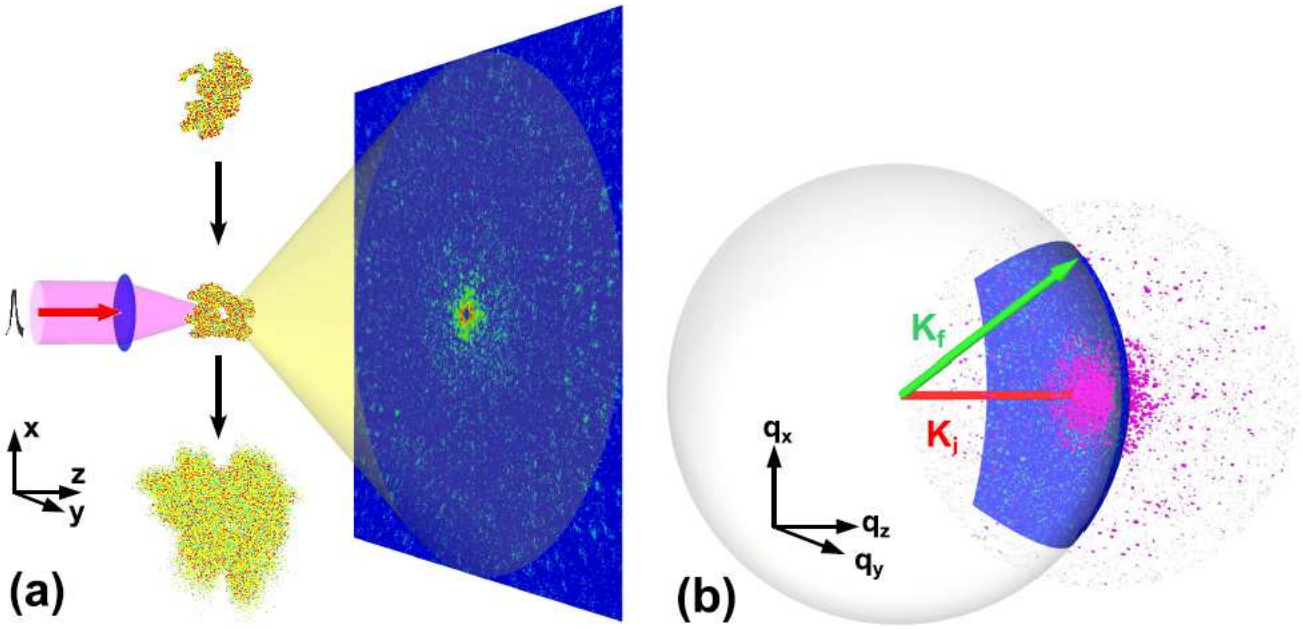

Fig. 31. (Color online) Schematic view of the experimental geometry. (a) In real space, diffraction pattern from a sample in random orientation is measured by a single FEL pulse. (b) In reciprocal space the measured diffraction pattern correspond to a cut of the 3D intensity distribution by an Ewald sphere sector. Vectors $\vec{K}_i$ and $\vec{K}_f$ denote the incident and diffracted wavevectors. Adapted form [80].

S2E Simulations of Bioimaging

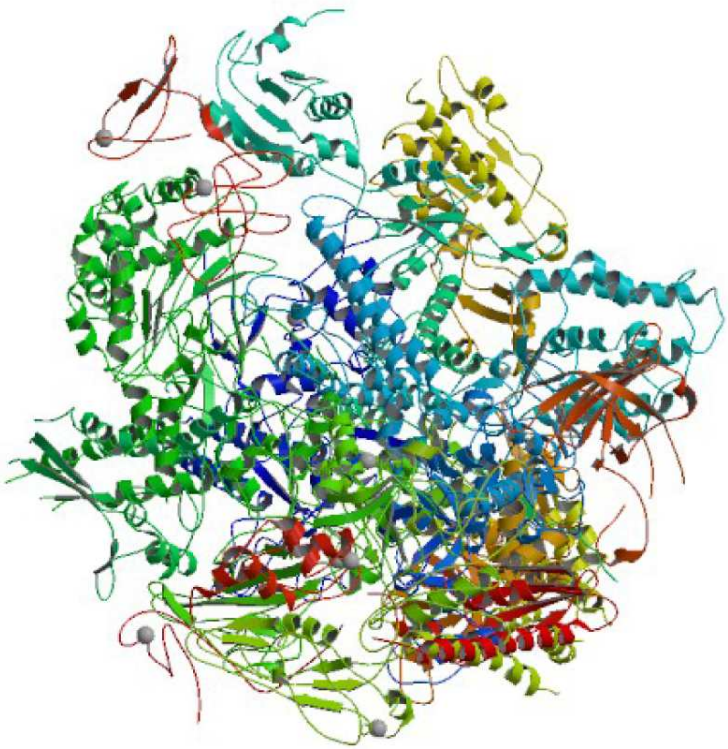

Fig. 32. Biological Assembly 1 of 1WCM - Complete 12-subunit RNA polymerase II at 0.38 nm, from [74].

S2E Simulations of Bioimaging

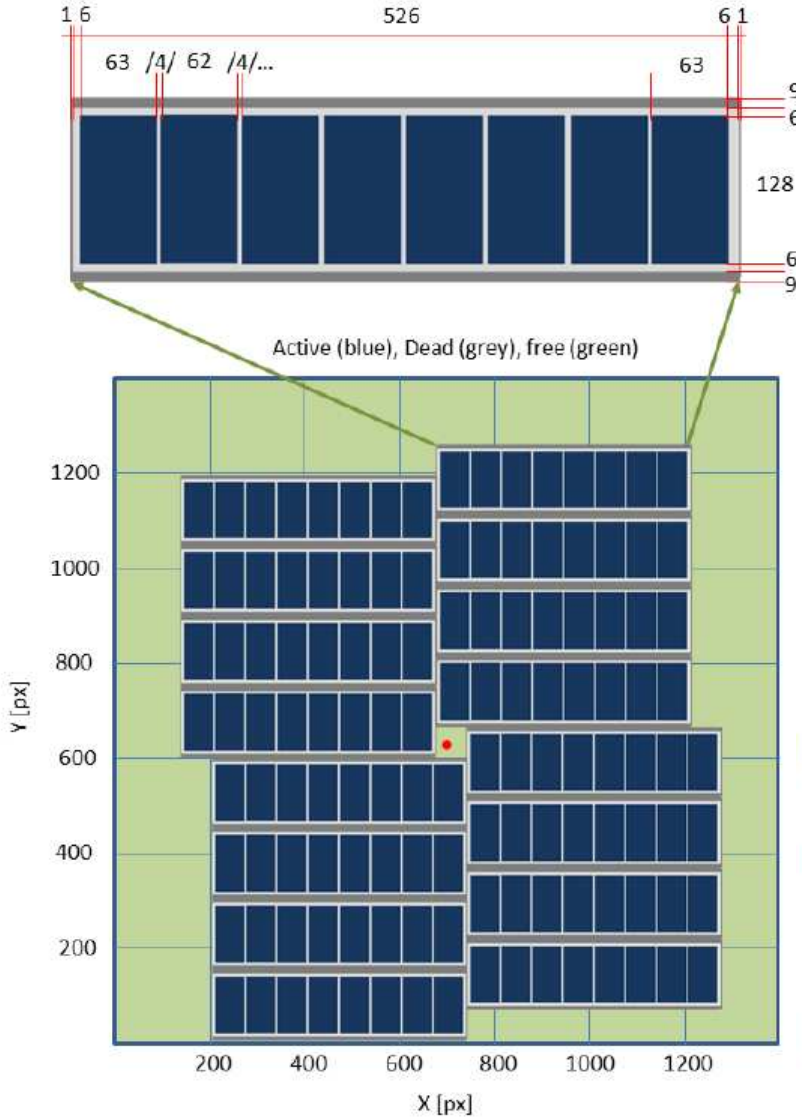

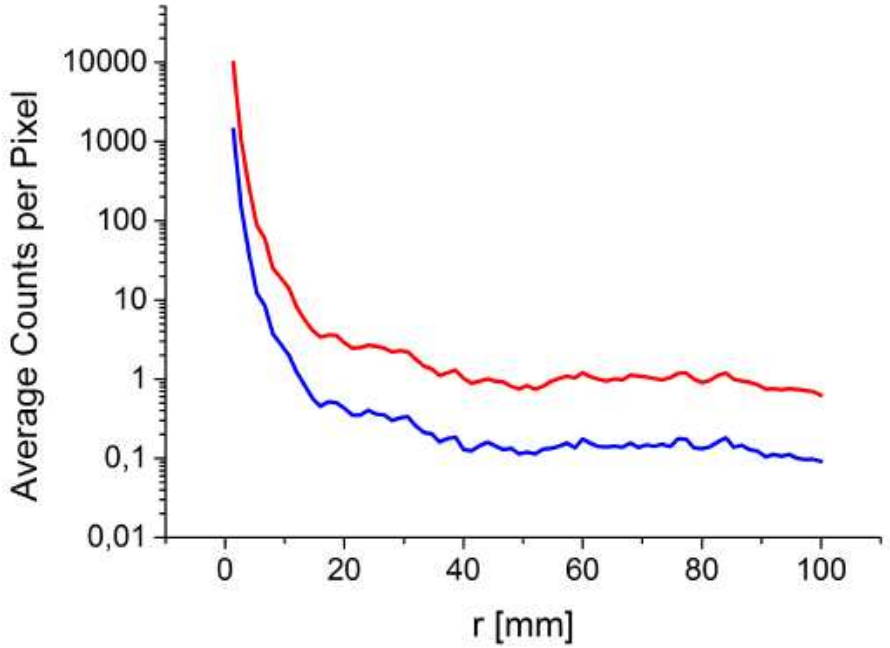

Fig. 35. Simulated diffraction data from RNA Pol II test object. The plots show the radial average of the photon counts per pixel. The simulations were performed at a photon energy of 4.1 keV. The detector considered here is 200 mm by 200 mm in size, and is located at a distance of 100 mm from the sample. The detector rim corresponds to 0.39 nm resolution. The pixel size is 1 mm. The pixel array has dimensions 200 by 200, corresponding to sampling $s = 2$ and binning $b = 5$. The blue line is for $0.15 \cdot 10^{23}$photons/cm^2, a fluence which can be achieved without changes of the SPB X-ray optics. The red line corresponds to 10^{23}photons/cm^2, a fluence which can be achieved with moderate modifications of the SBP X-ray optics.

S2E Simulations of Bioimaging

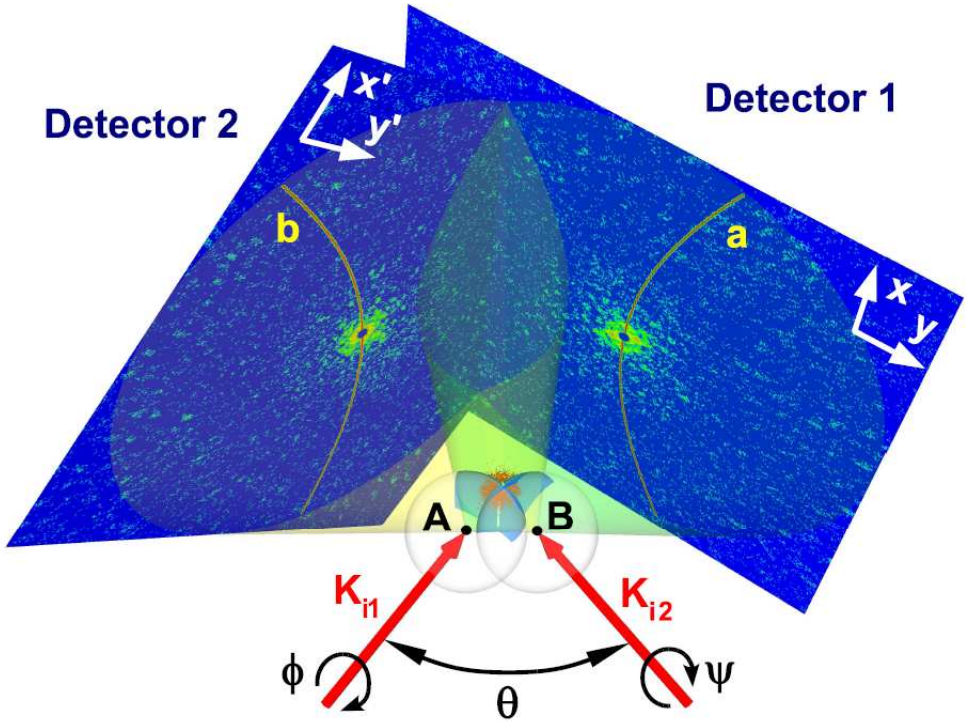

Fig. 37. (Color online) Measurements of two reproducible samples at random orientation can be considered as two measurements of the same sample with two different incident beam directions indicated by vectors $\vec{K}_{i1}$ and $\vec{K}_{i2}$. Angles ϕ, θ, ψ are Euler's rotation angles. Points A and B are the centers of the corresponding Ewald's spheres. Coordinates on the first and second detector are indicated as x, y and x', y', respectively. Adapted form [80].